JOURNAL OF CIVIL ENGINEERING AND MANAGEMENT
2010
16(4): 462–470

CURVATURE DUCTILITY PREDICTION OF REINFORCED HIGH-STRENGTH CONCRETE BEAM SECTIONS

Guray Arslan[1], **Ercan Cihanli**[2]

[1, 2]*Yıldız Technical University, Faculty of Civil Engineering,*
Civil Engineering Department, Structural Engineering Division,
34210 Davutpasa-Esenler-Istanbul-Turkey
E-mails: [1]*aguray@yildiz.edu.tr; gurayarslan@yahoo.com (corresponding author)*

Received 16 July 2009; accepted 9 June 2010

Abstract. The ductility of reinforced concrete beams is very important, since it is essential to avoid a brittle failure of the structure by ensuring adequate curvature at the ultimate limit state. One of the procedures used to quantify ductility is based on curvatures, namely, curvature ductility. It is necessary to know the curvature ductility of singly reinforced high-strength concrete (HSC) sections for determining a maximum permissible tensile reinforcement ratio or a maximum depth of the concrete compression area in design codes. The requirements of several codes and methods of prediction of the curvature ductility are based on the experimental results of normal strength concrete (NSC). The rules derived for NSC sections may not be appropriate for HSC sections, and verifications and modifications may be required for the evaluation of curvature ductility of HSC sections. In this study, the major factors affecting the curvature ductility of a singly reinforced HSC beam section are investigated. Based on numerical analyses, a parametric study has been carried out to evaluate the effects of various structural parameters on the curvature ductility of reinforced HSC beam sections.

Keywords: reinforced concrete, beam, curvature ductility, high-strength concrete, flexural strength, deformation.

1. Introduction

Although high-strength concrete (HSC) is often considered a relatively new material, its development has been gradual over many years (ACI 363R 1992). In recent years a marked increase in the use of HSC has been evident in construction projects around the world. HSC, $f_c > 50$ MPa, offers significantly better structural engineering properties, such as higher compressive and tensile strengths, higher stiffness, better durability, compared with conventional normal-strength concrete (NSC) (Mendis 2003). Experimental studies (Leslie *et al.* 1976; Kaar *et al.* 1978; Regan *et al.* 1993; Attard and Setunge 1996; Razvi and Saatcioglu 1999; Oztekin *et al.* 2003) have shown that significant differences exist in the stress-strain behaviors of NSC and HSC. Based on these studies, it is shown that concrete becomes increasingly more brittle as its compressive strength is increased. Despite HSC being a more brittle material compared with NSC, the curvature ductility for a specified reinforcement ratio of reinforced HSC section in flexure increases with the increase in the compressive strength of concrete (Park and Paulay 1975). Hence, HSC flexural members exhibit greater ductility, owing to lower neutral axis depths. This has been experimentally verified by Attard and Setunge (1996), Pendyala *et al.* (1996), Sarkar *et al.* (1997), Razvi and Saatcioglu (1999), Shin *et al.* (1999), Ashour (2000), Ko *et al.* (2001), Lin and Lee (2001).

Energy absorption capacities of reinforced concrete (RC) structural members depend on the level of ductility which is described in various ways. These include curvature, rotational, and displacement ductility (Cihanli and Arslan 2009). In order to provide a consistent level of minimum flexural ductility, an upper limit is generally set to ensure sufficient ductility at ultimate state, either by a maximum permissible tensile reinforcement ratio or by a maximum depth of the concrete compression area in design codes (TS 500 2000; ACI 318 2005; GBJ 11 1989; EN 1992:2004; NZS 3101 1995; BS 8110 1997). Ho *et al.* (2004) indicated that the values of section curvature ductility for NSC and HSC with the same upper limits are different, so it may be suggested for Codes that sections can be designed by setting minimum section curvature ductility for NSC and HSC. According to Leslie *et al.* (1976), to achieve the accustomed ductility in beams, ρ/ρ_b values should be limited to 0.35, for f_c in excess of 55MPa. Based on experimental results, Pam *et al.* (2001a) proposed to set a maximum limit to the tension steel to balanced steel ratio, whose values at different concrete strengths are given and developed a simple formula for predicting the ductility of beams.

Unconfined models developed for NSC may not be applicable to HSC. These models were shown to overestimate the strain of concrete at the peak stress and ductility when applied to HSC. Most of the models (Attard and Setunges 1996; Razvi and Saatcioglu 1999) proposed for HSC are modified versions of Hognestad's model deve-

ISSN 1392–3730 print / ISSN 1822–3605 online
doi:10.3846/jcem.2010.52

loped for NSC. Razvi and Saatcioglu's (1999) model can not be used for concrete having compressive strength higher than 108 MPa. Attard and Setunge's (1996) model is applicable to a broad range of concrete strength from 20 to 130 MPa but the extreme compression fiber of the unconfined concrete strain capacity is not limited. Hence, the values of curvature ductility and the ratio of ultimate neutral axis depth to the effective depth of section (x_u / d) are higher than the experimental values. Based on this evaluation (Cihanli and Arslan 2009), Hognestad's model (1951) is modified and the predictions of the model are compared with Ashour's (2000) experimental results. The comparisons of experimental and numerical results clearly show that the modified Hognestad's model (1951) is capable of accurately predicting the behavior of members subjected to flexure and evaluating the influence of various parameters on the curvature ductility of sections (Cihanli and Arslan 2009).

In order to provide a consistent level of minimum flexural ductility, it can be proposed to set a fixed minimum value for the curvature ductility factor. The minimum curvature ductility factor may be established by referring to the minimum curvature ductility factors being provided by the various existing codes, such as TS-500 (2000), ACI 318 (2005), GBJ 11 (1989), EN 1992:2004, NZS 3101 (1995) and BS 8110 (1997). According to Leet and Bernal (1997), curvature ductility ratios of 4 or more are typically considered desirable for reinforced concrete members that are subject to the large displacements and forces created by earthquakes. Knowledge of the curvature ductility is important for the design of beam sections. Using the results of 456 data for section, a parametric study has been carried out to evaluate the effects of various structural parameters on the curvature ductility and an alternative equation is proposed for predicting the curvature ductility of reinforced HSC beam sections.

2. Curvature ductility factor

Generally, the ductility is defined as the capacity of a material, section, structural element, or structure to undergo an excessive plastic deformation without a great loss in its load-carrying capacity. Rashid and Mansur (2005) used curvature ductility, μ_ϕ, defined as the ratio of curvature at failure to that at yield, instead of deflection ductility that is more difficult to calculate accurately. It is convenient to express the maximum curvature of beam sections in terms of this ductility factor. The curvature ductility of a RC section is expressed in the form of the curvature (μ_ϕ):

$$\mu_\phi = \frac{\phi_u}{\phi_y}, \tag{1}$$

in which ϕ_u and ϕ_y are the curvature at failure and at yielding of the tensile reinforcement, respectively. The ability of curvature ductility for singly reinforced sections is influenced by some factors such as the tensile reinforcement ratio, the compressive strength of concrete and yield strength of reinforcement, but the most important one is the tensile reinforcement ratio. Many researches have been conducted for studying the curvature ductility of RC sections (Ho *et al.* 2003, 2004; Lee and Pan 2003; Pam *et al.* 2001a, 2001b; Kwan *et al.* 2002). The equations defining the curvature ductility in some of those are summarized below.

Based on experimental results, Pam *et al.* (2001a) developed a simple formula for predicting the ductility of NSC and HSC beams. The following equation has been suggested:

$$\mu_\phi = 9.5(f_{cu})^{-0.30}\left(\frac{\rho}{\rho_b}\right)^{-0.75}, \tag{2}$$

in which f_{cu} is cube compressive strength of concrete.

According to Lee and Pan (2003), it is possible to devise a simple equation for the relationship between the curvature ductility and the tensile reinforcement ratio. The following equation has been suggested:

$$\rho = F\mu_\phi^G, \tag{3}$$

in which F and G are regression constants, tabulated for different material strengths and reinforcement ratios. However, F and G are expressed for only four concrete strengths (21, 28, 35 and 41 MPa), two reinforcement strengths (276 and 414 MPa) and five ratios of compressive reinforcement to tensile reinforcement (0.5, 0.6, 0.7, 0.8 and 0.9). Hence, this equation is not considered in the comparison of curvature ductility predictions.

Based on the regression analysis of the numerical results, Pam *et al.* (2001b) proposed the following equation for the prediction of the curvature ductility:

$$\mu_\phi = 10.7(f_c)^{-0.45}\left(\frac{\rho-\rho'}{\rho_b}\right)^{-1.25}\left(1+95.2(f_{co})^{-1.1}\left(\frac{\rho'}{\rho}\right)^3\right), \tag{4}$$

in which ρ_b, ρ' and ρ are the balanced reinforcement ratio, compressive reinforcement ratio and tensile reinforcement ratio, respectively. Assuming that the compressive reinforcement ratio is generally smaller than one quarter of the tensile reinforcement ratio and the last term in Eq. (4) is very close to 1.0, the ductility factor can be expressed as follows (Kwan *et al.* 2002):

$$\mu_\phi = 10.7(f_c)^{-0.45}\left(\frac{\rho-\rho'}{\rho_b}\right)^{-1.25}. \tag{5}$$

3. Moment-curvature analysis

It is important to know the details of stress-strain relationships of HSC in order to determine the full-range behavior of HSC members. Various stress-strain relationships for both unconfined and confined HSC under uniaxial compression have been proposed in the literature (Hongnestad 1951; Attard and Setunge 1996). In this study, concrete is assumed to be unconfined and the complete stress–strain (σ–ε) curve model which has been

shown to be applicable to range of concrete compressive strength higher than 50 MPa is adopted. Some regulations (Cihanli and Arslan 2009; Cihanli 2009) are made on the Hognestad's model for HSC using σ–ε relation obtained from numerical analyses. The σ–ε curve for ordinary concrete defined by Hognestad is given below (A-B curves in Fig. 1);

$$\sigma_c = f_c\left(\frac{2\varepsilon_c}{\varepsilon_{co}} - \left(\frac{\varepsilon_c}{\varepsilon_{co}}\right)^2\right), \tag{6}$$

in which ε_c and ε_{co} are strain of concrete and strain of concrete at the peak stress, respectively. HSC specimens are fractured suddenly (brittle failure) when they reach ultimate stress under uniaxial compression. Thus, to define the falling branch of σ–ε curve is not easy. According to Sarkar *et al.* (1997), the BS 8110 (1997) assumption of 0.0035 as the maximum usable concrete strain value seems to be high for the purpose of designing reinforced HSC members with compressive strength over 100 MPa. In the regulations on the Hognestad Model, the beam is assumed to be failed when the extreme compression fiber of the unconfined concrete core reaches a strain capacity $\varepsilon_{cu,\max}$, suggested by Ko *et al.* (2001) as

$$\varepsilon_{cu} = 0.003 + 1.44\frac{1}{f_c^2} + 0.00054\left(\frac{\rho'}{\rho}\right), \tag{7}$$

in which f_c is the compressive strength of concrete, ρ and ρ' are the ratio of tensile reinforcement and compressive reinforcement, respectively (C in Fig. 1). The strain of concrete at the peak stress ranges from about 0.002 to 0.003 for NSC and from about 0.003 to 0.0035 for lightweight concretes, the larger values in each case corresponding to the higher strength (Nilson 1997). In this model (Cihanli and Arslan 2009), the strain of concrete at the peak stress is expressed as follows (B in Fig. 1):

$$50 \text{ MPa} \le f_c \le 90 \text{ MPa},$$

$$\varepsilon_{co} = 0.002 + 0.001(f_c - 20)/70, \tag{8a}$$

$$f_c > 90 \text{ MPa}, \quad \varepsilon_{co} = 0.003. \tag{8b}$$

The post-peak branch becomes steeper as the strength increases (or ductility reduces). Lower strength concretes exhibit extensive ductility beyond maximum stress, so the energy absorption capacity is limited in HSC. The post-peak branch is expressed as follows (B-C curves in Fig. 1):

$$\sigma_c = f_c(1 - \psi(\varepsilon_c - \varepsilon_{co})), \tag{9}$$

$$50 \text{ MPa} \le f_c \le 90 \text{ MPa}$$

$$\psi = \frac{0.5 - 0.35(f_c - 40)/50}{\varepsilon_{cu} - \varepsilon_{co}}, \tag{10a}$$

$$f_c > 90 \text{ MPa} \quad \psi = 0.15/(\varepsilon_{cu} - \varepsilon_{co}). \tag{10b}$$

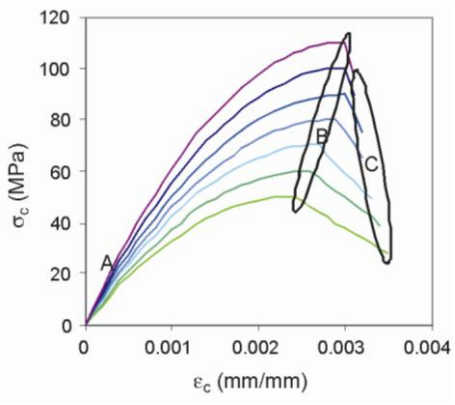

Fig. 1. Typical uniaxial stress-strain relationships for unconfined concrete

The relationship between concrete average principal tensile stress and strain is taken as linear elastic or parabolic up to cracking. A crack is assumed to initiate in a plane normal to the direction of the principal tensile strain once the principal tensile stress exceeds the concrete tensile strength, $f_{ct} = 0.3 f_c^{2/3}$ (EN 1992:2004; CST 49 1998). The σ–ε curve of concrete is described by a second-degree parabola (Ersoy and Ozcebe 2001),

$$0 \le \varepsilon_{ct} \le \varepsilon_{cto},$$

$$\sigma_{ct} = f_{ct}\left(\frac{2\varepsilon_{ct}}{0.0001} - \left(\frac{\varepsilon_{ct}}{0.0001}\right)^2\right) \le f_{ct}, \tag{11a}$$

or

$$\sigma_{ct} = 1000\varepsilon_{ct} \le f_{ct} \tag{11b}$$

in which σ_{ct} is the tensile stress of concrete, ε_{ct} and ε_{co} are the tensile strain of concrete in tension and tensile strain of concrete at the peak stress, respectively. After initiation of cracking, the σ–ε model follows a linear strain-softening branch intended to represent the post cracking tensile stress carried by concrete. The descending branch is linearly changing to a strain corresponding to $\varepsilon_{ctu} = 0.0002$.

$$\varepsilon_{cto} \le \varepsilon_{ct} \le \varepsilon_{ctu}$$

$$\sigma_{ct} = f_{ct} - \frac{f_{ct}}{\varepsilon_{ctu}}(\varepsilon_{ct} - 0.0001) \ge 0.5 f_{ct}. \tag{12}$$

The σ–ε relationship used for reinforcing steel consists of three segments. The elastic and yield portions of the curve form a bilinear relationship. The strain hardening portion is represented by a parabolic curve and follows the yield segment. A perfect bond is assumed between concrete and steel reinforcement and steel reinforcement is assumed to carry only axial loads. Reinforcing steels having yield strengths of 220, 420 and 530 MPa are used in analyses.

Three basic assumptions are made in the numerical analyses, that: a) plane sections before bending remain plane after bending; b) the tensile strength of the concrete may be neglected; c) there is no bond-slip between the

reinforcement bars and the concrete. The moment–curvature behavior of the beam section is obtained by calculating moment and curvature for various values of compressive strain at the extreme fiber of concrete. Based on the above assumptions, the stresses developed have to satisfy the axial equilibrium condition, from which the neutral axis depth is evaluated by iteration. Having determined the neutral axis depth, the resisting moment is calculated from the moment equilibrium condition. The calculations are performed by dividing the section into rectangular strips (Yalcin and Saatcioglu 2000; Ersoy and Ozcebe 2001; Cihanli and Arslan 2009). This procedure is repeated until the maximum compressive strain of concrete reaches the value of ε_{cu} or when the strain of the tensile reinforcement reaches the value of $\varepsilon_{su} = 0.10$ and 0.16 for $f_y = 420,$ 530 and 220 MPa, respectively.

4. Development of an alternative curvature ductility prediction equation

Based on the numerical analyses results (Cihanli and Arslan 2009), it can be observed that the use of the three important variables ρ/ρ_b, f_c and f_y should be incorporated for developing an alternative equation for the curvature ductility of sections (μ_ϕ). The first step is to determine the basic format of the curvature ductility equation using parametric study. The resulting function is as follows:

$$\mu_\phi = kf\left(\frac{\rho}{\rho_b}; f_c; f_y\right), \tag{13}$$

in which k is the constant. The balanced reinforcement ratio (ρ_b) is taken as (ACI 318 2005)

$$\rho_b = 0.85\beta_1 \frac{f_c}{f_y}\frac{600}{600+f_y} \text{ (MPa)}, \tag{14}$$

in which β_1 is defined as

$$\beta_1 = 0.85 - 0.008(f_c - 30) \geq 0.65 \text{ for } f_c > 30 \text{ MPa}, \tag{15a}$$

$$\beta_1 = 0.85 \text{ for } f_c \leq 30 \text{ MPa}. \tag{15b}$$

In numerical analyses, minimum ratio of tension reinforcement is taken as (Turkish Earthquake Code 2007)

$$\rho \geq 0.8 f_{ct}/f_y, \tag{16}$$

where f_{ct} is the tensile strength of concrete in MPa and equals to $0.35\sqrt{f_c}$.

4.1. Parametric study

A parametric study is undertaken to identify the influence of three parameters on the curvature ductility of RC beam sections, which are computed numerically, and to define the factor k and the function in Eq. (13) more precisely. Numerical results were compared to Ashour's (2000) experiments in Cihanli and Arslan (2009), and it was observed that they are in good agreement. The section dimensions are the same as those of Ashour's (2000) experimental beams, where the width, total depth and effective depth of beam section are 200, 250 and 215 mm, respectively. They represent typical singly reinforced sections. Numerical analyses are carried out by varying compressive strength of concrete (f_c) from 50 to 110 MPa at increments of 5 MPa, tensile reinforcement ratio (ρ) from 0.0059 to 0.0708 at increments of 0.0059 and yield strength of reinforcement (f_y) for 220, 420 and 530 MPa.

$$\mu_\phi = k\left(\frac{\rho}{\rho_b}\right)^{b1} (f_c)^{b2} (f_y)^{b3}. \tag{17}$$

The exponents b1, b2 and b3, and the coefficient k in Eq. (17) are determined from multiple regression analysis. The effect of each parameter is studied by varying its magnitude while maintaining the other variables constant. For each case, the value of the curvature ductility (μ_ϕ) is computed numerically and the development of the exponents is determined from multiple regression analyses.

4.2. Influence of ρ/ρ_b on curvature ductility

The results of numerical analyses for f_y = 420~530 MPa, f_c = 48~110 MPa and $\rho/\rho_b = 0.0755 \sim 1.2708$ indicate that the curvature ductility decreases as ρ/ρ_b increases for singly reinforced HSC sections.

In order to ensure sufficient ductility, all the structural elements should be correctly reinforced: the detailed rules created for that purpose, especially in codes of practice, should be respected (Bernardo and Lopes 2004). The most commonly used means of guaranteeing adequate ductility is to limit the tensile reinforcement ratio, ρ. According to the Turkish Code (TS-500 2000) and ACI 318R (2005) Building Code, in flexural members, ρ should be limited to $0.85\rho_b$ and $0.75\rho_b$, respectively. The results of numerical analyses for $f_c \geq 50$ MPa indicate that the curvature ductility decreases while ρ/ρ_b increases. The reduction in the curvature ductility can be explained by the increase in the neutral axis depth, resulting in a lower tensile force. Based on the numerical results for twelve series of ρ/ρ_b, the effects of the all variables are evaluated collectively.

A regression analysis is undertaken to identify the influence of ρ/ρ_b on the curvature ductility using the results of numerical analyses. The effect of ρ/ρ_b on the curvature ductility is illustrated in Fig. 2, which shows that the proposed equation matches closely with the numerical results of curvature ductility. The ρ/ρ_b has a pronounced effect on the curvature ductility. The results of numerical analyses show that the curvature ductility

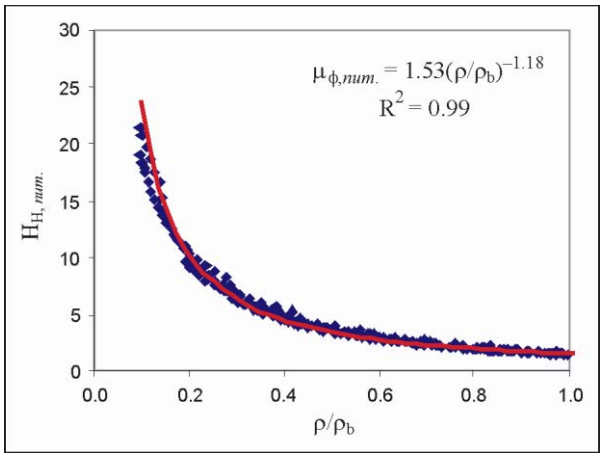

Fig. 2. Influence of ρ/ρ_b on the curvature ductility

decreases with increase in ρ/ρ_b, though not proportionally. Based on this parametric study, the variation of curvature ductility of RC sections can be expressed as

$$\mu_{\phi,num} = 1.53\left(\frac{\rho}{\rho_b}\right)^{-1.18} . \qquad (18)$$

Eq. (18) indicates that ρ/ρ_b increases as a result of decreasing curvature ductility. Compared to the ACI code, this equation also indicates that for the same curvature ductility, ρ/ρ_b increases with decreasing curvature ductility.

4.3. The influence of compressive strength of concrete on curvature ductility

The results of numerical analyses for f_y = 420~530 MPa, f_c = 50~110 MPa and $\rho/\rho_b = 0.0755 \sim 1.2708$ are evaluated, and the change of curvature ductility with the compressive strength of concrete is studied.

Higher-strength concrete is more brittle, and its ultimate strain capacity of extreme compression fiber is less than that of lower-strength concrete. Based on numerical analyses, Rashid and Mansur (2005) indicated that ductility increases first with an increase in concrete strength, reaching a maximum value at f_c = 105 MPa. Thereafter, any increase in concrete strength leads to a decrease in ductility. Concrete strength corresponding to this optimum ductility, however, is not the same as that observed experimentally. Nevertheless, the analysis supports the experimental trend (Rashid and Mansur 2005).

A regression analysis is undertaken to identify the influence of compressive strength of concrete on the curvature ductility using the results of numerical analyses. The variation of the numerical curvature ductility of singly RC sections ($\mu_{\phi,num.}$) with the ρ/ρ_b can be expressed as follows,

$$\frac{\mu_{\phi,num.}}{(\rho/\rho_b)^{-1.18}} = 3.28\, f_c^{-0.17} . \qquad (19)$$

This equation clearly shows that the curvature ductility is expressed as a function of $(f_c)^{-0.17}$. The effect of compressive strength of concrete on curvature ductility and $(\rho/\rho_b)^{-1.18}$ is illustrated in Fig. 3.

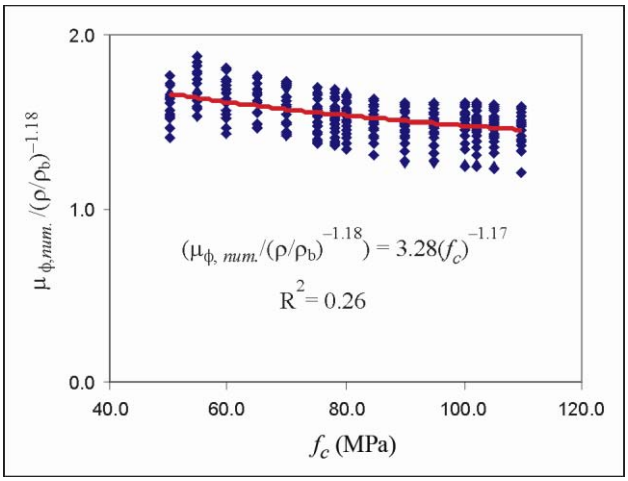

Fig. 3. Influence of f_c on the ratio of curvature ductility to $(\rho/\rho_b)^{-1.18}$

4.4. Influence of yield strength of reinforcement on curvature ductility

Pam *et al.* (2001a) proposed Eq. (2), which ignores the effect of the yield strength of the steel on the ductility, by considering 20 beams with the yield strength of the steel ranging from 519 MPa to 579 MPa. In the analyses, it is aimed to capture the relationship between the curvature ductility and the yield strength of the steel. The results of numerical analyses for f_c = 70 MPa, $\rho/\rho_b = 0.0917 \sim 1.2182$, and f_y = 220, 420 and 530 MPa indicate that the curvature ductility decreases as f_y increases.

A regression analysis is undertaken to identify the influence of yield strength of reinforcement on the curvature ductility of HSC sections using the results of numerical analyses. The variation of the numerical curvature ductility of singly RC sections ($\mu_{\phi,num.}$) with f_c and the ρ/ρ_b can be expressed as follows,

$$\frac{\mu_{\phi,num.}}{\left(\frac{\rho}{\rho_b}\right)^{-1.18}(f_c)^{-0.17}} = 41.63(f_y)^{-0.42} . \qquad (20)$$

This equation clearly shows that the curvature ductility is expressed as a function of $(f_y)^{-0.42}$. The effect of yield strength of reinforcement (f_y) on the curvature ductility is illustrated in Fig. 4, which shows that the proposed equation matches closely with the numerical results.

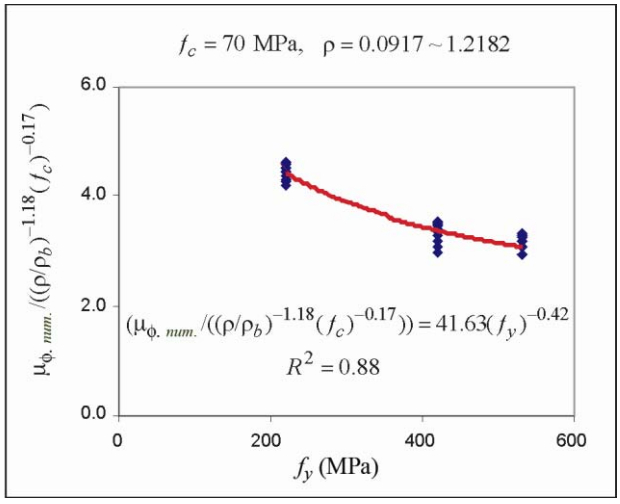

Fig. 4. Influence of f_y on the ratio of curvature ductility to $(\rho/\rho_b)^{-1.18}(f_c)^{-0.17}$

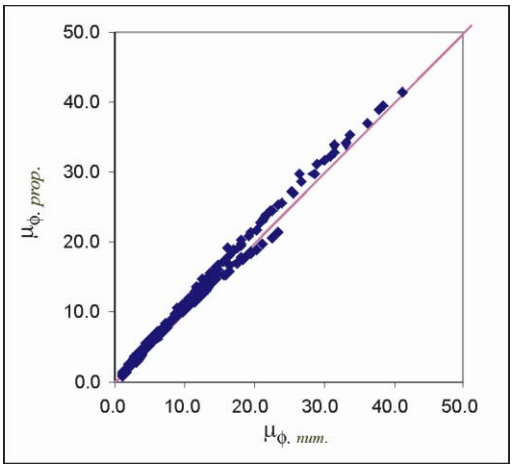

Fig. 5. Proposed curvature ductility values using Eq. (21) versus numerical analysis results

5. Proposed curvature ductility equation for unconfined RC beams

Based on the previous parametric study, considering the influence of parameters; the ratio of tensile reinforcement to balanced reinforcement (ρ/ρ_b), the compressive strength of concrete (f_c) and yield strength of reinforcement (f_y), on the proposed curvature ductility ($\mu_{\phi,prop.}$) can be expressed as

$$\mu_{\phi,prop.} = 40\left(\frac{\rho}{\rho_b}\right)^{-1.18}(f_c)^{-0.17}(f_y)^{-0.42}, \quad (21)$$

in which f_c is the concrete cylinder strength (MPa) and f_y is the yield strength of reinforcement (MPa).

6. Evaluation of proposed equation

The proposed curvature ductility in Eq. (21) captures the effect of change in the ρ/ρ_b, f_c and f_y on the numerical results. The results obtained numerically are compared with Pam's *et al.* (2001a) predictions by Eq. (2), Kwan's *et al.* (2002) predictions by Eq. (5), and the proposed equation given by Eq. (21).

Fig. 5 compares the proposed curvature ductility obtained from Eq. (21) with the numerical results. It can be observed that the proposed curvature ductility values are in good agreement with the numerical results. Based on the results for 456 sections with reinforcement yield strengths 220, 420 and 530MPa, mean value(MV) and standard deviation(SD) for the ratio of the proposed curvature ductility obtained from Eq. (21) to the numerical result are 0.935 and 0.052, respectively. Based on the same sections, MV and SD for the ratio of the Pam's *et al.* (2001a) prediction by Eq. (2) to the numerical result are 1.137 and 0.193, respectively and MV and SD for the ratio of the Kwan's *et al.* (2002) prediction by Eq. (5) to the numerical result are 0.931 and 0.060, respectively.

Fig. 6 show the errors which can be induced by the discrepancy of f_c, ρ/ρ_b, f_y and ρ between the numerical results and the proposed curvature ductility values by Eq. (21). The ratio of the results obtained from Eq. (21) to the numerical results is not significantly influenced with increased f_c, but it is influenced with changes in ρ/ρ_b and ρ. The discrepancy between the numerical results and the results obtained from Eq. (21) increases for $\rho/\rho_b < 0.2$ and $\rho/\rho_b > 1.0$. The same behavior is observed for $0.01 < \rho < 0.03$.

Table 1 shows the comparison of the curvature ductility values obtained numerically with the Pam's *et al.* (2001a) predictions by Eq. (2), the Kwan's *et al.* (2002) predictions by Eq. (5) and the proposed equation given by Eq. (21). It can be seen that the proposed Eq. (21) results in the lowest coefficient of variation (COV) and hence it provides better results than the Pam's *et al.* (2001a, b) and the Kwan's *et al.* (2002) predictions of curvature ductility, based on the comparisons with the numerical results.

By testing the proposed curvature ductility Eq. (21) against 159 numerical results for f_y = 220 MPa, the COV obtained for the ratio of proposed Eq. (21) to numerical result is 15% of that obtained using Pam's *et al.* (2001a) prediction by Eq. (2) and 51% of that obtained using Kwan's *et al.* (2002) prediction by Eq. (5).

By testing the proposed curvature ductility equation Eq. (21) against 160 numerical results for f_y = 420 MPa, the COV obtained for the ratio of proposed Eq. (21) to numerical result is 21% of that obtained using Pam's *et al.* (2001a) prediction by Eq. (2) and 59% of that obtained using Kwan's *et al.* (2002) prediction by Eq. (5).

By testing the proposed curvature ductility equation Eq. (21) against 137 numerical results for f_y = 530 MPa, the COV obtained for the ratio of proposed Eq. (21) to numerical result is 21% of that obtained using Pam's *et al.* (2001a) prediction by Eq. (2) and 59% of that obtained using Kwan's *et al.* (2002) prediction by Eq. (5).

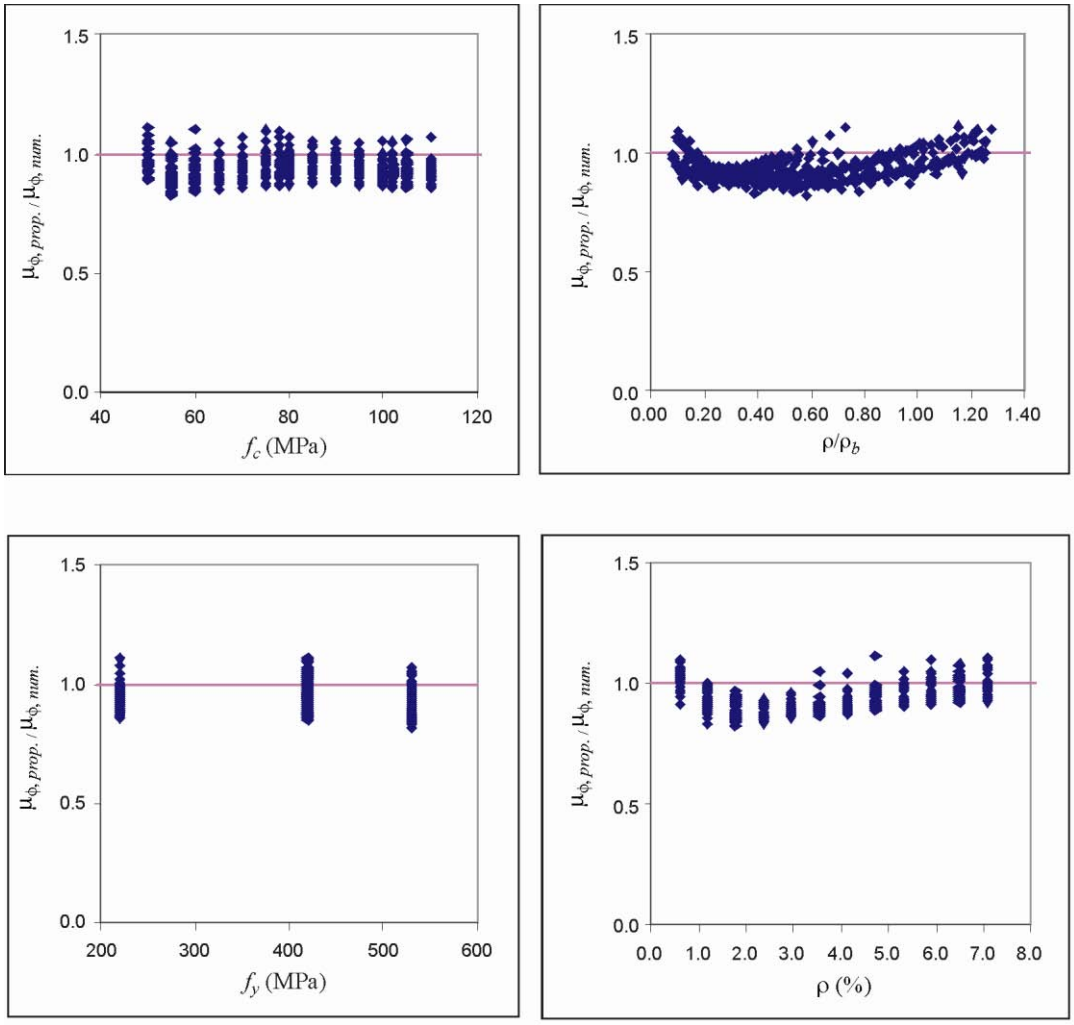

Fig. 6. Comparing curvature ductility on proposed Eq. (21) with numerical analysis results for various f_c, ρ/ρ_b, f_y and ρ

Table 1. Verification of curvature ductility predictions

	f_y = 220 MPa			f_y = 420 MPa			f_y = 530 MPa		
	MV	SD	COV	MV	SD	COV	MV	SD	COV
Prop. Eq. (21)/Num.	0.933	0.036	0.039	0.952	0.056	0.059	0.918	0.055	0.060
Pam's *et al*. (2001a)/Num.	0.725	0.193	0.266	1.304	0.374	0.286	1.419	0.398	0.281
Kwan's *et al*. (2002)/Num.	0.780	0.060	0.077	0.991	0.099	0.100	1.038	0.106	0.102
Num.= Numerical									

It is worthy to note that the ductility definitions developed by Pam *et al.* (2001a, b) and Kwan *et al.* (2002) were based on moment-deflection and moment-curvature curves, respectively.

7. Conclusions

The predictions obtained from the proposed curvature ductility equation, Pam's *et al.* (2001a, b) equation and Kwan's *et al.* (2002) equation have been compared with the existing results of numerical analyses. The following conclusions can be drawn from the results of this study.

By testing the proposed curvature ductility equation Eq. (21) against 456 numerical results for all reinforcement yield strengths, the COV obtained for the ratio of proposed Eq. (21) to numerical result is 33% of that obtained using Pam's *et al.* (2001a) prediction by Eq. (2) and 85% of that obtained using Kwan's *et al.* (2002) prediction by Eq. (5).

Based on the results of the numerical analyses, a simple equation is recommended for the prediction of the curvature ductility considering, ρ/ρ_b, f_c and f_y.

The curvature ductility can be conveniently predicted using the proposed Eq. (21) but further calibrations with the results of numerical analyses of RC beam sections are needed to obtain a better performance.

References

ACI Committee 318. Building code requirements for reinforced concrete (ACI318–05) and commentary (ACI318R–05). American Concrete Institute (ACI), 2005, Detroit, Mich.

ACI Committee 363R–92. State-of-the-Art Report on High-Strength Concrete, Reported by ACI Committee 363, Re-approved 1997, Farmington Hills, MI.

Ashour, S. A. 2000. Effect of compressive strength and tensile reinforcement ratio on flexural behavior of high-strength concrete beams, *Engineering Structures* 22(5): 413–423. doi:10.1016/S0141-0296(98)00135-7

Attard, M. M.; Setunge, S. 1996. The stress–strain relationship of confined and unconfined concrete, *ACI Materials Journal* 93(5): 432–444.

Bernardo, L. F. A.; Lopes, S. M. R. 2004. Neutral axis depth versus flexural ductility in high-strength concrete beams, *Journal of Structural Engineering* 130(3): 452–459. doi:10.1061/(ASCE)0733-9445(2004)130:3(452)

British Standards Institution, Part 1: Structural Use of Concrete: Code of Practice for Design and Construction, BSI, London. 1997. BS 8110.

Chinese Academy of Building Research, Seismic Design Code for Buildings and Structures. Chinese Academy of Building Research, Beijing. 1989. GBJ 11.

Cihanli, E.; Arslan, G. 2009. Curvature ductility of unconfined reinforced high strength concrete beam sections, *Journal of Engineering and Natural Sciences* 27: 139–150 (in Turkish).

Cihanli, E. 2009. *The flexural behavior of high-strength concrete beams*: Ms Thesis. Yıldız Technical University, Istanbul (in Turkish).

Concrete Society Technical (CST) Report 49. Design guidance for high strength concrete. United Kingdom, 1998. 168 p.

Ersoy, U.; Ozcebe, G. 2001. *Reinforced concrete.* Evrim Yayınevi (in Turkish).

Eurocode 2. Design of Concrete Structures, Part 1–1. General rules and rules for buildings, EN 1992–1–1. December, 2004. European Committee for Standardization. 2004.

Ho, J. C. M.; Kwan, A. K. H.; Pam, H. J. 2003. Theoretical analysis of post-peak flexural behaviour of normal and high strength concrete beams, *The Structural Design of Tall and Special Buildings* 12: 109–125. doi:10.1002/tal.216

Ho, J. C. M.; Kwan, A. K. H.; Pam, H. J. 2004. Minimum flexural ductility design of high strength concrete beams, *Magazine of Concrete Research* 56(1): 13–22.

Hognestad, E. 1951. *A study of combined bending and axial load in reinforced concrete members.* Bull. Ser. No. 399, University of Illinois, Engineering Experimental Station, Urbana, Ill.

Kaar, P. H.; Hanson, N. W.; Capel, H. T. 1978. Stress-strain characteristics of high strength concrete structure, *ACI SP–55*: 161–185. Detroit.

Ko, M. Y.; Kim, S. W.; Kim, J. K. 2001. Experimental study on the plastic rotation capacity of reinforced high strength concrete beams, *Materials and Structures* 34: 302–311. doi:10.1007/BF02482210

Kwan, A. K. H.; Ho, J. C. M.; Pam, H. J. 2002. Flexural strength and ductility of reinforced concrete beams, *Proceedings of the ICE – Structures and Buildings* 152(4): 361–369.

Lee, T. K.; Pan, A. D. E. 2003. Estimating the relationship between tension reinforcement and ductility of reinforced concrete beam sections, *Engineering Structures* 25(8): 1057–1067. doi:10.1016/S0141-0296(03)00048-8

Leet, K. M.; Bernal, D. 1997. *Reinforced concrete design.* The McGraw-Hill Co, Inc. 3rd ed.

Leslie, K. E.; Rajagopalan, K. S.; Everard, N. J. 1976. Flexural Behavior of High-Strength Concrete Beams, *ACI Journal* 73(9): 517–521.

Lin, C. H.; Lee, F. S. 2001. Ductility of high performance concrete beams with high strength lateral reinforcement, *ACI Structural Journal* 98(4): 600–608.

Mendis, P. 2003. Design of high-strength concrete members: state-of-the-art, *Progress in Structural Engineering and Materials* 5(1): 1–15. doi:10.1002/pse.138

New Zealand standard code of practice for the design of concrete structures (NZS 3101). Standard Association of New Zealand (NZS). 1995. Wellington, New Zealand.

Nilson, A. H. 1997. *Design of Concrete Structures*. McGraw-Hill İnternational Editions, 12th ed.

Oztekin, E.; Pul, S.; Husem, M. 2003. Determination of rectangular stress block parameters for high performance concrete, *Engineering Structures* 25(3): 371–376. doi:10.1016/S0141-0296(02)00172-4

Pam, J. H.; Kwan, A. K. H.; Islam, M. S. 2001a. Flexural strength and ductility of reinforced normal-and high-strength concrete beams, *Proceedings of the ICE – Structure and Buildings* 146(4): 381–389.

Pam, H. J.; Kwan, A. K. H.; Islam, M. S. 2001b. Post-peak behavior and flexural ductility of doubly reinforced high-strength concrete beams, *Structural Engineering and Mechanics* 12(5): 459–474.

Park, R.; Paulay, T. 1975. *Reinforced Concrete Structures.* John Wiley and Sons, New York, 195–269. doi:10.1002/9780470172834.ch6

Pendyala, R.; Mendis, P.; Patnaikuni, I. 1996. Full-range behavior of high strength concrete flexural members: comparison of ductility parameters of high and normal-strength concrete members, *ACI Structural Journal* 93(1): 30–35.

Rashid, M. A.; Mansur, M. A. 2005. Reinforced high-strength concrete beams in flexure, *ACI Structural Journal* 102(3): 462–471.

Razvi, S.; Saatcioglu, M. 1999. Confinement model for high-strength concrete, *Journal of Structural Engineering ASCE* 125(3): 281–289. doi:10.1061/(ASCE)0733-9445(1999)125:3(281)

Regan, P. E.; Al-Hussaini, A. A.; Ramdane, K. E.; Xue, H. Y. 1993. Behaviour of high strength concrete slabs, in *Proceedings of Concrete 2000 International Conference*, University of Dundee, V. 1, E&FN Spon, Cambridge, UK, 1: 761–773.

Sarkar, S.; Adwan, O.; Munday, J. G. L. 1997. High strength concrete: an investigation of the flexural behaviour of high strength RC beams, *The Structural Engineer* 75(7): 115–121.

Shin, S. W.; Yoo, S. H.; Ahn, J. M.; Lee, K. S. 1999. The ductile behaviour including flexural strength of high-strength concrete members subjected to flexure, *ACI Special Publication* 172: 247–280.

TS-500 Requirements for design and construction of reinforced concrete structures. Turkish Standards Institute. Ankara, Turkey. 2000 (in Turkish).

Turkish Earthquake Code for Buildings, Ministry of Public Works and Resettlement. Ankara, Turkey. 2007 (in Turkish).

Yalcin, C.; Saatcioglu, M. 2000. Inelastic analysis of reinforced concrete columns, *Computers and Structures* 77(5): 539–555. doi:10.1016/S0045-7949(99)00228-X

STIPRIOJO BETONO SIJŲ SKERSPJŪVIO PLASTIŠKUMO KREIVĖS PROGNOZĖ

G. Arslan, E. Cihanli

Santrauka

Gelžbetoninių sijų plastiškumas yra labai svarbi savybė, apsauganti konstrukciją nuo staigios irties. Tam užtikrinti reikalinga atitinkama kreivė, esant tinkamumo ribiniam būviui. Plastiškumas įvertinamas naudojant kreivines diagramas – plastiškumo kreives. Norint nustatyti didžiausią tempiamos armatūros kiekį arba didžiausią gniuždomosios zonos aukštį, remiantis normomis reikia žinoti armuoto stipriojo betono (HSC) plastiškumo kreivę. Kai kurios normos ir metodai plastiškumo kreivę nustato pagal paprastojo betono (NSC) eksperimentinius duomenis. Taisyklės, skirtos paprastojo betono skerspjūvio plastiškumo kreivei nustatyti, gali netikti stipriajam betonui, todėl reikia atlikti papildomus tyrimus ir metodų pakeitimus. Šiame darbe tiriami pagrindiniai veiksniai, darantys įtaką stipriojo betono plastiškumo kreivei. Atliekant skaitinį modeliavimą, buvo įvertinti įvairūs skerspjūvio konstrukciniai parametrai, darantys poveikį stipriojo betono plastiškumo kreivei.

Reikšminiai žodžiai: gelžbetonis, sija, plastiškumo kreivė, stiprusis betonas, stiprumas lenkiant, deformacija.

Guray ARSLAN. An Associate Professor at the Department of Civil Engineering, Yıldız Technical University. He received his PhD from the University of Yıldız Technical, Istanbul, Turkey. His main research interest is the behavior of reinforced concrete members under monotonic and cyclic actions.

Ercan CIHANLI. Civil Engineer. He received his Ms Degree from the University of Yıldız Technical, Istanbul, Turkey. His main research interest is the behavior of reinforced concrete beams under bending.